

# A new estimate of the extragalactic $\gamma$ -ray background as seen by EGRET

I. A. Grenier<sup>a</sup>, J. M. Casandjian<sup>a</sup>, R. Terrier<sup>b</sup>

(a) AIM (CEA/Paris 7/CNRS), UMR 7158, Service d'Astrophysique, CEA Saclay, 91191 Gif/Yvette, France

(b) APC (Paris 7/CNRS/CEA), UMR 7164, 11 place Marcelin Berthelot, 75005 Paris, France

Presenter: I. Grenier (isabelle.grenier@cea.fr), fra-grenier-I-abs1-og21-oral

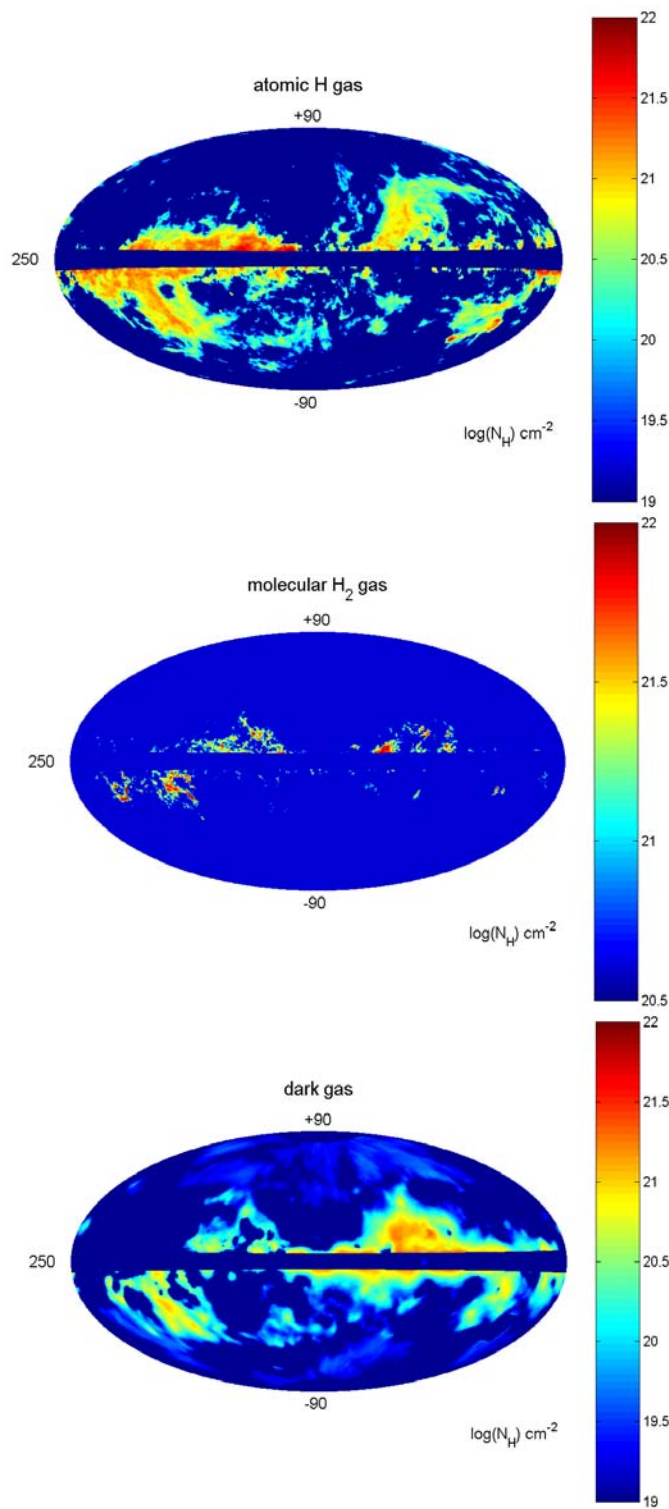
Large amounts of dark gas, not accounted for in the HI and CO surveys, have been found in infrared and  $\gamma$  rays above 100 MeV at the interface between the atomic and molecular clouds in the solar neighbourhood. The local measurements imply a total dark-gas mass in the Milky Way at least comparable to the molecular mass detected in CO. The column-densities and large angular extent of the local dark clouds imply severe revisions of the  $\gamma$ -ray interstellar emission model to high latitudes. A new estimate of the extragalactic  $\gamma$ -ray background intensity is presented, but we point out large systematic uncertainties due to our limited knowledge of the foreground emissions, in particular the contributions from the nearby radio loops and the local inverse Compton (IC) emission.

## 1. Modelling the local interstellar $\gamma$ radiation

The Milky Way is a bright, diffuse source of high-energy  $\gamma$  rays that are produced in cosmic-ray interactions with interstellar gas and radiation. An accurate, detailed model of this emission is important to detect point-sources and to measure the extragalactic  $\gamma$ -ray background (EGRB) in the 0.03-10 GeV energy band. Several models are available in the Galactic disc, based on different assumptions about the cosmic-ray distribution [1, 2, 3]. In the  $5^\circ \leq |b| \leq 80^\circ$  latitude interval of interest here, most of the interstellar emission arises within a kpc where the cosmic-ray density appears to be rather uniform [4, 5]. So, the  $\gamma$ -ray emission can be modelled as a linear combination of the total gas column-densities, the Galactic IC intensity ( $I_{IC}$ ), an isotropic background intensity ( $I_B$ ), and the point-sources.

The recent comparison of gas tracers in the solar neighbourhood, such as the HI and CO lines from the atomic and molecular gas, the dust total column-densities or reddening derived from its 94-3000 GHz thermal emission, and the  $\gamma$  rays from cosmic-ray interactions, has led to the discovery of large amounts of “dark gas” which are not accounted for in the HI and CO surveys [5]. The dark gas is traced in  $\gamma$  rays and by its dust content. Its gas-to-dust ratio is equivalent to that in the CO clouds. It forms large clouds surrounding all the dense molecular cores detected in CO and reaching out to the more extended HI clouds of the local medium. The dark and HI gas occupy comparable volumes. Figure 1 shows that the hydrogen column-densities in the 3 phases are similar. The diffuse H<sub>2</sub> or dense HI nature of the dark gas is still unclear. There are enough grains and shielding to form H<sub>2</sub> molecules, but they may be too sparse to efficiently excite the CO lines since the average volume densities (in molecules) in the dark gas are typically 10 times less than in the CO phase. On the other hand, the dark gas could be dense, optically thick, atomic gas, as commonly found in the HI self-absorption studies. An extrapolation of the local measurements to the Milky Way, using the CO mass spectrum for Galactic clouds and the  $M_{dark} \propto M_{CO}^{0.4}$  found locally, implies a total dark-gas mass in the Galaxy at least comparable to that detected in CO [5].

To account for the different contributions to the  $\gamma$ -ray emission (neglecting the H<sup>+</sup> one) and their distinct spatial distributions, we have modelled the EGRET photon count maps,  $N_\gamma(E, l, b)$  with  $0.5^\circ$  bin size, in several energy bands as:



$$N_\gamma(E,l,b) = q_{\text{SOU}}(E).N_{\text{SOU}}(l,b) + \epsilon(E,l,b) \times [q_{\text{HI}}(E).N_{\text{HI}}(l,b) + q_{\text{CO}}(E).W_{\text{CO}}(l,b) + q_{\text{EBV}}(E).R_{\text{EBV}}(l,b) + q_{408}(E).I_{408}(l,b) + q_{\text{IC}}(E).I_{\text{IC}}(l,b) + I_B(E)].$$

The EGRET archival database provides 4-year P1234 count maps and exposure maps  $\epsilon(E,l,b)$  in 10 energy bands from 30 MeV to 10 GeV.  $N_{\text{SOU}}$  notes the count map expected from the point-sources that have been detected above the new interstellar emission model in the P1234 data above 500 MeV [6]. The  $N_{\text{HI}}$  column-densities were derived from the recent Leiden/Argentine/Bonn data for a spin temperature of 120 K [7]. The velocity-integrated CO brightness temperature map,  $W_{\text{CO}}$ , comes from the CfA compilation at  $|b| \leq 32^\circ$  [8]. The dust reddening  $E(B-V)$  map comes from the 100 $\mu\text{m}$  and 240 $\mu\text{m}$  data from IRAS and DIRBE after correction to a uniform temperature of 18.2 K [9]. The residual dust map,  $R_{\text{EBV}}$ , obtained after removal of the  $E(B-V)$  part linearly correlated with  $N_{\text{HI}}$  and  $W_{\text{CO}}$ , traces the dark clouds [5]. The 408 MHz map [10] traces GeV electrons to high latitudes. They can up-scatter the ambient soft radiation to  $\gamma$  rays. Those trapped in the nearby radio loops may also produce bremsstrahlung radiation in the gas shells. The brightness temperature of  $3.7 \pm 0.85$  K of the isotropic radio background due to the cosmological microwave background and the unresolved radio sources has been removed from the 408 MHz map [11]. All interstellar maps were convolved with the instrument PSF for an input 2.1 spectral index. The model was fitted to the  $\gamma$ -ray data by means of a maximum-likelihood test with Poisson statistics.

**Figure 1.** Maps, in Galactic coordinates centered on  $l=70^\circ$ , of the  $N(\text{HI})$ ,  $2N(\text{H}_2)$ , and  $N(\text{H}_{\text{dark}})$  column-densities found in the nearby clouds.  $N(\text{H}_2)$  is computed from the  $W_{\text{CO}}$  data using the  $X_\gamma$  ratio measured locally above 100 MeV. The three phases are closely associated in space and exhibit comparable column-densities.

The model was fitted to the whole sky data at latitudes  $5^\circ \leq |b| \leq 80^\circ$  in order to constrain the largest-scale components, such as the Galactic IC radiation and emission from the nearby radio electrons. Table 1 gives the best fit results above 100 MeV, with their statistical errors, for models with and without the contribution from the radio electrons. Systematic uncertainties are discussed in detail in [12, 13]. The use of the new and better calibrated HI data yields a slightly lower  $q_{\text{HI}}$  emissivity, thus a higher  $X_\gamma = N(\text{H}_2)/W(\text{CO}) = q_{\text{CO}}/2q_{\text{HI}} = (1.97 \pm 0.04) 10^{20} \text{ cm}^{-2} \text{ K}^{-1} \text{ km}^{-1}$  ratio, than previous local estimates [5]. The significant increase in the likelihood ratio resulting from the addition of the 408 MHz map ( $2\ln\lambda = 267$ ) strongly suggests that the GeV electrons in Loop I and Loop III radiate in  $\gamma$  rays. This increase remains very significant at  $15^\circ \leq |b| \leq 80^\circ$  ( $2\ln\lambda = 194$ ). The IC and/or bremsstrahlung origin of the emission will be investigated.

**Table 1.** Best fit to the EGRET data at  $5^\circ \leq |b| \leq 80^\circ$ ,  $E > 100$  MeV

$q_{\text{HI}}$	$q_{\text{CO}}$	$q_{\text{EBV}}$	$q_{\text{I408}}$	$q_{\text{IC}}$	$q_{\text{SOU}}$	$I_B$
$10^{-26} \text{ s}^{-1} \text{ sr}^{-1}$	$10^{-6} \text{ cm}^{-2} \text{ sr}^{-1}$ $\text{K}^{-1} \text{ km}^{-1}$	$10^{-6} \text{ mag}^{-1}$ $\text{cm}^{-2} \text{ s}^{-1} \text{ sr}^{-1}$	$10^{-7} \text{ K}^{-1} \text{ cm}^{-2}$ $\text{s}^{-1} \text{ sr}^{-1}$	%	%	$10^{-6} \text{ cm}^{-2} \text{ s}^{-1} \text{ sr}^{-1}$
$1.23 \pm 0.01$	$4.86 \pm 0.10$	$49.6 \pm 1.6$	$1.93 \pm 0.17$	$56.4 \pm 1.6$	$98 \pm 1$	$11.61 \pm 0.28$
$1.29 \pm 0.01$	$5.12 \pm 0.10$	$50.1 \pm 1.6$		$72.9 \pm 0.7$	$99 \pm 1$	$13.8 \pm 0.1$

Note:  $I_B$  values of  $(14.5 \pm 0.5) 10^{-6}$  and  $(11.1 \pm 0.1) 10^{-6} \text{ cm}^{-2} \text{ s}^{-1} \text{ sr}^{-1}$  were obtained for the ‘EGRET’ [12] and ‘GALPROP’ [13] models, respectively, for  $E > 100$  MeV.

## 2. Determining the extragalactic $\gamma$ -ray background spectrum

The extragalactic  $\gamma$ -ray background is most difficult to determine because its derivation relies on modelling foregrounds that are not firmly established. Table 1 and Figure 2 illustrate that its overall intensity and spectrum depend within 50 % on the choice of model.

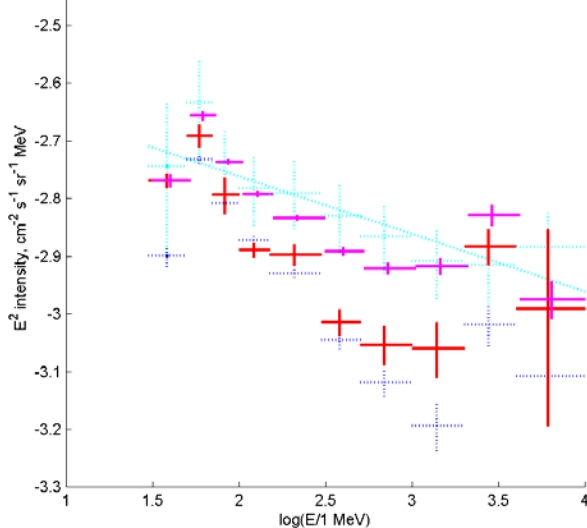


**Figure 2.** Spectrum of the isotropic  $\gamma$  radiation obtained with (red) and without (magenta) use of the radio template in the foreground model, compared with the ‘EGRET’ [cyan, 12] and ‘GALPROP’ [blue, 13] estimates. The errors are purely statistical. The dashed cyan line corresponds to the differential  $2.743 10^{-3} E^{-2.1} \text{ cm}^{-2} \text{ s}^{-1} \text{ MeV}^{-1}$  fit to the ‘EGRET’ estimate. Energies are slightly shifted for clarity.

Sreekumar et al. [12] have used the first 3 years of EGRET data and the standard ‘EGRET’ model for Galactic emission [2] with HI and CO gas, and IC emission based on the local electron spectrum and smooth dust and stellar distributions in the Galactic disc. Strong et al. [13] have used 4 years of EGRET data and their optimized ‘GALPROP’

model for cosmic-ray propagation which is constrained by several diagnostics ( $\gamma$  and radio maps, local spectra of protons, antiprotons, positrons and abundance ratios). We have used the same 4 years

of data, a local gas model that includes new HI and CO data as well as the dark clouds that subtend large solid angles on the sky, the Galactic IC emission maps from a newer version of GALPROP [14], and a possible additional contribution from nearby electrons traced in radio.

Without the 408 MHz template, we find an isotropic spectrum in good agreement with the ‘EGRET’ model. Their closeness suggests that the gas-related foregrounds, visible as well as dark, are efficiently removed, despite well-known non-linearities in the gas tracers. Adding the distribution of synchrotron emitting electrons to the foreground model, on top of the Galactic IC component, has a significant impact. The isotropic intensity drops by 15% and the spectrum steepens. It is indeed expected that IC emission from local electrons upscattering the cosmological microwave background and interstellar radiation largely contributes to the isotropic  $\gamma$ -ray component, but it is very difficult to determine its absolute proportion and spectrum. Their density, spectrum, and scale height above the Galactic plane are highly uncertain. An anisotropic, large angular scale, electron population is trapped in Loop I and Loop III. An even more diffuse population, isotropic or at angular scales larger than the giant radio loops, is indicated by the large offset temperature ( $T_b \sim 8K$ ) of the radio map above the extragalactic radio background. So, for limited variations of the local magnetic field, the radio map crudely traces their relative  $\gamma$ -ray contribution compared to that of electrons in the Galactic disc and nearby loops. These diffuse electrons have a dominant impact on the EGRB. The resulting EGRB estimate compares well with the more sophisticated ‘GALPROP’ one. It is worth noting that the latter used the electron spectrum measured at Earth, but multiplied by a factor of 4.

The measured spectrum is not consistent with an  $E^{-2.1}$  power law, but shows some positive curvature. Yet, the visible softening at low energy, in particular below 150 MeV, may be due to the wide instrumental PSF and the resulting significant degeneracy between the HI, IC and exposure maps that cause an artificial increase in the isotropic component. The instrument sensitivity below 70 MeV is also uncertain by 20%. A large fraction of the EGRB is expected from unresolved sources, primarily from blazars, possibly from galaxy clusters, starbursts galaxies, and hard  $\gamma$ -ray burst events, yet the predictions span a broad range from 25% to 100%. The hard spectrum found at medium and high energy with GALPROP and our local foreground modelling is consistent with a dominant blazar origin. Given the systematic uncertainties in the foregrounds, in particular in the local IC spectrum [1], as well as visible instrumental effects in the residual maps that could not be removed, the hardening above 2 GeV should not be taken too literally, especially in terms of annihilation of weakly interacting massive particles.

## References

- [1] A. W. Strong, I. V. Moskalenko, O. Reimer, *Astrophys. J.* 613, 962 (2004).
- [2] S. D. Hunter et al., *Astrophys. J.* 481, 205 (1997)
- [3] A. W. Strong, J. R. Mattox, *Astron. Astrophys.* 308, L21 (1996)
- [4] S. Digel, I. A. Grenier, S. D. Hunter, T. M. Dame & P. Thaddeus, *Astrophys. J.* 555, 12 (2001)
- [5] I. A. Grenier, J. M Casandjian, R. Terrier, *Science* 307, N°5713, 1292 (2005)
- [6] J. M. Casandjian, I. A. Grenier, these proceedings
- [7] P. M. W. Kalberla et al., *Astron. Astrophys.*, in press (2005)
- [8] T. M. Dame, D. Hartmann, P. Thaddeus, *Astrophys. J.* 547, 792 (2001).
- [9] D. J. Schlegel, D. P. Finkbeiner & M. Davis, *Astrophys. J.* 500, 525 (1998).
- [10] C. G. T. Haslam, C. J. Salter, H. Stoffel, W. E. Wilson, *Astron. Astrophys. Suppl. Ser.* 47, 1 (1982)
- [11] P. Reich, W. Reich, *Astron. Astrophys. Suppl. Ser.* 74, 7 (1988)
- [12] P. Sreekumar et al., *Astrophys. J.* 494, 523 (1998)
- [13] A. W. Strong, I. V. Moskalenko, O. Reimer, *Astrophys. J.* 613, 956 (2004).
- [14] A. W. Strong, I. V. Moskalenko, O. Reimer, S. Digel, R. Diehl, *Astron. Astrophys.* 422, L47 (2004).